mixture of 1% ceric ammonium sulfate in 85% phosphoric acid. If the color reagent is diluted with an equal volume of water, it is more conveniently sprayed; however, more than one spraying may be required with the diluted reagent to obtain sharp and stable colored zones. Table II shows the colors obtained, the ultraviolet characteristics, and the R_f values of the alkaloids in the two systems desiccatot discussed above.

Some precautions have been necessary to obtain the best results. The plates should be oven-dried at 105° for at least 30 minutes before using them. The dried plates may be stored for weeks in a suitable desiccator without noticeable effects on their performance. Color development is best if the plates are heated to 100° immediately after they are removed from the chamber and are kept warm for at least 5 minutes before spraying them. As mentioned above, the diluted color reagent is the best for the detection purposes in spite of the necessity of repeated sprayings. The colors are quite stable overnight if the plate is kept warm (90–100°) and no moisture is allowed to come into contact with the plate. The colors fade considerably if the plate is allowed to cool and absorb moisture from the air. The color development will be poor if the spraying is delayed more than 30 minutes after removing the plate from the solvent system, even though the plate is kept warm.

REFERENCES

(1) Cone, J. N., Miller, R., and Neuss, N., THIS JOURNAL, 52, 688 (1963).
(2) Gorman, M., Neuss, N., Svoboda, G. H., Barnes, A. J., Jr., and Cone, N. J., *ibid.*, 48, 256(1959).
(3) Gorman, M., Neuss, N., and Svoboda, G. H., *J. Am. Chem. Soc.*, 81, 4745(1959).
(4) Gorman, M., Neuss, N., and Biemann, K., *ibid.*, 84, 1058(1962).
(5) Jakovljevic, I. M., THIS JOURNAL, 51, 187(1962).
(6) Johnson, I. S., Wright, H. F., Svoboda, G. H., and Vlantis, J., *Cancer Res.*, 20 (7), 1016(1960).
(7) Neuss, N., Gorman, M., Svoboda, G. H., Maciak, G., and Beer, C. T., *J. Am. Chem. Soc.*, 81, 4754(1959).
(8) Neuss, N., Gorman, M., Boaz, H. E., and Cone, N. J., *ibid.*, 84, 1509(1962).
(9) Svoboda, G. H., Gorman, M., Neuss, N., and Barnes, A. J., Jr., THIS JOURNAL, 50, 409(1961).
(10) Svoboda, G. H., *Lloydia*, 24, 173(1961).
(11) Svoboda, G. H., Johnson, I. S., Gorman, M., and Neuss, N., THIS JOURNAL, 51, 707 (1962).
(12) Svoboda, G. H., *ibid.*, 52, 407(1963).

____ *Technical Articles* ____

New Rheometer for Determining Rheological and Viscoelastic Properties of Fluids

By DUNCAN E. McVEAN* and JERE E. GOYAN‡

A rising cylinder rheometer is described which can be used to study the flow properties of fluids in the low shear regions similar to those caused by a falling particle. The rheometer may also be used to study viscoelastic properties of fluids. The rheometer was used to obtain flow curves in the low shear region of several pharmaceutical suspending agents. Bingham yield values were obtained by extrapolating methods from these flow curves. Dynamic viscosities of these materials were obtained by analysis of their relaxation behavior. The dynamic viscosities are compared with the plastic viscosities of the materials in the low shear range.

THE COMMONLY used suspension vehicles exhibit either pseudoplastic or plastic flow properties (1). Flow curves for these fluids over a wide range of shear rates may be obtained from viscometers currently in use (2).

However, the measurement of shearing forces at the very low shear rates produced by a falling particle is difficult to obtain with available viscometers. An example of the magnitude of desirable shear may be obtained as follows. Consider a 100-μ particle with a density of 2.00 falling in a Newtonian fluid having a density of 1.00 and a viscosity of 10 poise. The maximum shear rate (at the equator of the sphere) will be 0.16 reciprocal seconds. It was therefore decided to build a viscometer which could produce viscometric data at these low shear rates. An additional advantage to such an instrument would be the more precise determination of yield value obtainable because of the shorter extrapolation to zero shear rate.

The development of a new viscometer seemed desirable because of the difficulties that would be

encountered in modifying instruments now in use. Frictional forces encountered at low r.p.m. negate the use of coaxial cylinder rotational viscometers. Slattery (3) has shown in his study of the flow of non-Newtonian materials around a sphere that the use of falling sphere instruments would yield data requiring complex computations in order to extract viscometric data. Experiments involving capillary instruments are both time consuming and inefficient when used to study non-Newtonian materials.

An instrument which seemed ideally suited for low shear measurements of non-Newtonian materials is the translated cylinder (Pochettino) viscometer (4). Several authors have discussed and used this type of instrument (5–9). Bergen and Patterson (10) modified the instrument using a closed tube with a solid cylindrical bob. This enabled them to obtain very low shear rates. Unfortunately, the flow in such a closed system is complex; large correction factors were needed with their instrument.

Description of the Rheometer.—In general the instrument designed in this laboratory consists of a cylinder rising in a tube open at both ends; both tube and cylinder are immersed in the sample. A schematic diagram of the rheometer is presented in Fig. 1. The tube was selected by examining several lengths of tubing and choosing one which deviated from being round by no more than 0.005 cm. The supports for the tube consist of two sets of three stainless steel tapered fingers.

Since the tube is open at both ends, the complex flow patterns associated with closed-end tubes are avoided. The cylinder is raised at a uniform velocity through the liquid being studied. The resistance of the material to the motion of the cylinder through it is recorded with a strain gauge.
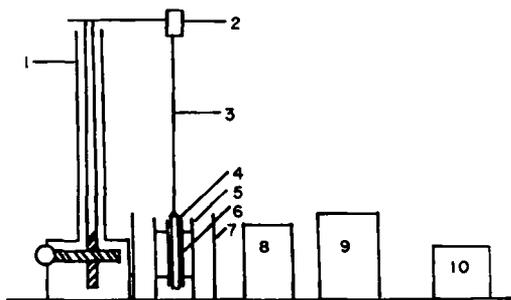

Fig. 1.—The rising cylinder rheometer. Key: *1*, lifting mechanism, Gardner tensile strength apparatus, Gardner Laboratory, Bethesda, Md.; *2*, Statham transducer, G1-1.5-350, Statham Instruments, Hato Rey, Puerto Rico; *3*, Coats and Clark's O.N.T. extra strong button and carpet cord, S. S. Kresge Co.; *4*, 12.70 × 0.4302-cm. stainless steel cylindrical rod or bob; *5*, 15.88 × 5.08-cm. stainless steel sample container; *6*, 10.16 × 0.4646-cm. hollow stainless steel tube or cup; *7*, temperature controlled water bath; *8*, motor controller, GT 21, G. K. Heller Co., Las Vegas, Nev.; *9*, transducer amplifier-indicator, 311, Sanborn Co., Waltham, Mass.; *10*, Varian recorder, G-10, Varian Associates, Instrument Div., Palo Alto, Calif.

The diameter of the sample container was large with respect to the diameter of the cup to minimize the error due to flow of the liquid through the annulus between the cup and the walls of the container. The water bath, tensile strength apparatus, and motor are all mounted on a stainless steel plate attached to a vibradamp.[1] The rates of shear were 0.166, 0.219, 0.304, and 0.434 seconds^{-1}. Nearly vibrationless stirring of the water bath was accomplished with a centrifugal pump.[2] Temperature was maintained at 30 ± 0.1°.

The equations necessary for the instrument may be derived as

$$\eta = \frac{F}{dS/dt} = (\text{dyne-sec. cm.}^{-2}) \quad (\text{Eq. 1})$$

where η is viscosity, F is the force per unit area on the cylinder (shear stress), and dS/dt is the rate of
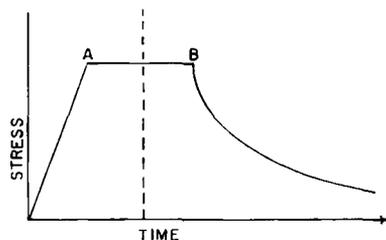

Fig. 2.—A typical upcurve for a non-Newtonian fluid is shown to the left of the dotted line. Point *A* represents the point where steady-state flow begins. Point *B* to the right of the dotted line represents the beginning of relaxation following cessation of steady-state flow. The dotted line signifies several minutes of elapsed time.

shear. *F* is computed from the following (11)

$$F = \left[\frac{2\pi h \eta}{\ln (R_T/R_C)}\right] V_{avg} \quad (\text{Eq. 2})$$

where h = length of the cylinder, R_C = radius of the cylinder, R_T = radius of the tube, and V_{avg} = the average velocity of the fluid flow in the annulus. V_{avg} is related to the rate of rise of the cylinder through

$$V_{avg} = V \left\{ \left[\frac{R_C \ln R_C - R_T \ln R_T - R_C + R_T}{[\ln (R_T/R_C)] (R_T - R_C)}\right] \right.$$
$$\left. + \frac{\ln R_T}{\ln (R_T/R_C)} \right\} \quad (\text{Eq. 3})$$

where V is the rate of rise of the cylinder in cm. seconds^{-1}. Further calculations show that the shear stress (dynes cm.$^{-2}$) for the rising cylinder rheometer is

$$F = \frac{Wg}{2\pi h R_C} = 71.204 \ W \quad (\text{Eq. 4})$$

where W is the recorded force in grams, and g is the gravitational acceleration with substitution of the dimensions of the instrument providing the final equality. The rate of shear strain (seconds^{-1}) is

$$\frac{dS}{dt} = \frac{V_{avg}}{\ln (R_T/R_C)} \frac{1}{R_{avg}} = 26.61 \ V_{avg} \quad (\text{Eq. 5})$$
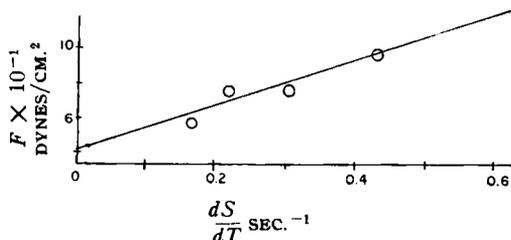
Fig. 3.—Viscosity curve of tragacanth initial mucilage determined by the rising cylinder rheometer with intercept being the Bingham yield value.

a mixer[5] for 1 hour. Then the solution was allowed to stand for 1 hour to release the entrapped air. The ammonia was added slowly with mixing to neutralize the Carbopol 934 and to convert it into its mucilagenous form. This mucilage was diluted to produce mucilages of concentrations 0.10, 0.15, 0.23, and 0.30% (w/v).

EXPERIMENTAL

The cylinder was uniformly raised 15 mm. through a sample producing an upcurve such as shown in Fig. 2. It should be noted that steady-state flow

TABLE I.—YIELD VALUES (DYNES/CM.^{2}) FOR TRAGACANTH AND CARBOPOL 934 MUCILAGES

			Tragacanth			Carbopol 934		
				Super				
No. 1	No. 2	A	Initial	Initial	Supreme	0.10%	0.15%	0.23%
23.0	14.5	16.6	42.4	156.4	123.4	1.7	16.8	131.1

TABLE II.—VALUES OF THE APPARENT VISCOSITY IN POISE AT LOW RATES OF SHEAR FOR TRAGACANTH AND CARBOPOL 934 MUCILAGES

			Tragacanth				Carbopol 934		
				Super					
Sec.$^{-1}$	No. 1	No. 2	A	Initial	Initial	Supreme	0.10%	0.15%	0.23%
0.166	211.4	126.5	206.6	380.1	1469.8	966.9	8.1	73.1	660
0.219	178.5	105.9	182.6	321.9	1232.9	785.8	7.8	70.9	595
0.304	149.7	83.9	161.2	267.8	1036.2	631.6	7.2	68.1	490
0.434	127.0	73.0	145.2	227.6	884.8	511.5	6.5	61.4	325

where R_{avg} is the radius of the midpoint of the annulus between the tube and the cylinder.

Solving Eq. 2 for η yields the equation for viscosity proposed by Fox and Flory (12) for a Pochettino type viscometer

$$\eta = \frac{(F/2\pi h)\,[\ln\,(R_T/R_C)]}{V_{avg}} \qquad \text{(Eq. 6)}$$

After substitution of the dimensions of the instrument, Eq. 6 becomes

$$\eta = 2.5761\,(W/V_{avg}) \qquad \text{(Eq. 7)}$$

Likewise, Eq. 3 becomes

$$V_{avg} = 0.4449\,V \qquad \text{(Eq. 8)}$$

Materials.—Six samples of powdered tragacanth gum U.S.P. were obtained from the S. B. Penick Co. The samples were identified as tragacanth No. 1, No. 2, A, Initial, Super Initial, and Supreme. Mucilages were prepared according to the following formula: tragacanth powder, 20 Gm.; benzoic acid, 1 Gm.; glycerin, 60 ml.; and purified water, 1000 ml.

The water and glycerin were mixed, heated to boiling, and the benzoic acid was dissolved in them. This was followed by sprinkling the powdered gum tragacanth on the boiling solution. After boiling for 5 minutes, the mixtures were agitated at intervals during the next 48 hours. After hydrating for 68 hours, the mucilages were homogenized.[3]

A stock solution of Carbopol 934[4] was also prepared according to the formula: ammonia (28% in water), 7 Gm.; Carbopol 934 powder, 10 Gm.; and distilled water, 983 ml. The Carbopol 934 powder and the distilled water were mixed with

occurred almost immediately. The value of the force at which steady-state flow occurs is dependent upon the apparent viscosity of the sample and the particular rate of rise selected.

To compare this instrument with another viscometer, the viscosity of Karo syrup was obtained using the M-2 viscometer (13); it was 11.218 poise. The viscosity of the syrup determined by the rising cylinder instrument was 11.517 poise. This was considered a satisfactory agreement.

Figure 2 also presents a representation of a typical downcurve or stress relaxation curve obtained from the rising cylinder rheometer after cessation of steady-state flow. The stress was allowed to relax at constant strain for 9380 seconds or until it became zero.

The resisting force upon the cylinder at each rate of shear was converted to dynes cm.$^{-2}$ with Eq. 4. Then these values were plotted *versus* the rate of shear strain to give a flow curve for each mucilage in the low shear range. Figure 3 is an example of one such curve.

The plotted points appeared to be linear and did not pass through the origin. These points were therefore fitted to a straight line by the method of least squares, the intercept of the line with the stress axis being taken as the classical Bingham yield value for the material. The yield values for each of these mucilages determined by the above methods are listed in Table I. The apparent viscosity of the mucilages at each rate of shear are found in Table II.

Since the relaxation of stress within the sample at constant strain could easily be determined, it was decided to analyze these data to see if additional information could be obtained about the behavior of the samples. Examination of stress

TABLE III.—RELAXATION OF STRESS IN THE RISING CYLINDER RHEOMETER AND THE RELAXATION SPECTRA FOR 2% TRAGACANTH SUPER INITIAL MUCILAGE

Time, Sec.	0.166 Sec.$^{-1}$ σ dynes cm.^{2}	H dynes cm.^{2}	0.219 Sec.$^{-1}$ σ dynes cm.^{2}	H dynes cm.^{3}	0.304 Sec.$^{-1}$ σ dynes cm.^{2}	H dynes cm.^{2}	0.434 Sec.$^{-1}$ σ dynes cm.^{2}	H dynes cm.^{2}
0	223.65	...	271.56	...	335.51	...	459.44	...
0.38	215.32	177.43	261.89	163.50	326.54	1446.09	347.97	108.90
0.76	205.21	221.89	247.72	16.39	309.52	108.92	330.24	108.90
1.14	194.10	192.27	238.03	122.20	287.45	241.66	311.87	99.83
1.52	183.92	155.31	223.87	203.17	264.67	217.81	293.43	88.49
1.90	167.26	283.95	208.20	195.77	236.18	290.22	271.93	217.82
2.28	150.67	236.62	193.25	136.05	202.79	242.08	248.07	181.52
2.66	137.71	177.07	178.29	186.30	175.09	165.87	222.73	109.07
3.04	125.68	123.86	159.71	203.82	154.73	108.90	199.73	163.47
3.42	120.12	118.10	141.77	181.28	141.70	72.62	169.75	145.35
3.80	112.79	48.71	133.58	130.46	131.94	39.95	149.03	87.13
7.60	83.17	24.35	76.83	24.48	88.79	14.53	92.14	16.34
11.40	72.98	13.31	62.66	12.22	73.27	9.72	75.26	7.26
15.20	64.72	8.86	53.69	8.15	64.37	6.34	69.14	4.78
19.00	58.24	1.77	46.28	8.96	59.46	5.08	61.45	3.26
38.00	52.69	1.78	40.30	1.22	44.79	0.36	47.64	1.10
57.00	46.21	1.19	35.82	0.54	39.87	0.24	44.57	0.36
76.00	45.29	1.10	29.83	0.20	37.45	0.90	44.57	0.11
234.50	27.70	0.23	22.36	0.19	27.70	0.12	29.98	0.01
1172.50	9.26	0.08	14.95	0.03	24.42	0.01	26.92	0
2345.00	9.26	0	14.95	0.01	21.15	0	23.07	0
4690.00	0	...	14.95	0	16.31	...	22.29	...
7035.00	...	...	14.95	...	9.75	...	21.50	...
9380.00	...	...	14.95	...	8.12	...	0	...

relaxation is usually visualized in terms of a model consisting of a spring and dashpot in series (14). Under constant strain the force on the spring (at any time t) must be equal and opposite to the force on the dashpot. Since the element does not change length during the experiment

$$\frac{\dot{\sigma}}{G} = -\frac{\sigma}{\eta} \qquad \text{(Eq. 9)}$$

where σ = stress in the spring, $\dot{\sigma}$ = rate of change of stress in the spring, η = viscosity of dashpot liquid, and G = spring modulus.

Solving with the boundary condition $\sigma = \sigma_0$ at zero time

$$\sigma = \sigma_0 e^{-t/\tau} \qquad \text{(Eq. 10)}$$

where $\tau = \eta/G$

Any real liquid will appear to have many such models in parallel leading to

$$\sigma = l\Sigma_i G_i e^{-t/\tau i} \qquad \text{(Eq. 11)}$$

where $\tau_i = \eta_i/G_i$ and l is the elongation.
Now σ/l may be defined as $G(t)$, then

$$G(t) = \Sigma_i G_i e^{-t/\tau i} \qquad \text{(Eq. 12)}$$

Allowing i to increase without limit,

$$G(t) = \int_{-\infty}^{\infty} G(\tau) e^{-t/\tau} d\tau \qquad \text{(Eq. 13)}$$

or

$$G(t) = \int_{-\infty}^{\infty} \tau G(\tau) e^{-t/\tau} d\ln \tau \qquad \text{(Eq. 14)}$$

$$= \int_{-\infty}^{\infty} H(\tau) e^{-t/\tau} d\ln \tau \qquad \text{(Eq. 15)}$$

where $H(\tau) \equiv \tau G(\tau) \equiv H$ is called the relaxation spectrum.

When the rising cylinder is stopped abruptly during steady-state flow, the shear rate just prior to cessation of flow will be defined as $(\dot{\gamma})_0$. Solving Eq. 9 with this boundary condition

$$\sigma = \eta \dot{\gamma}_0 e^{-t/\tau} = \dot{\gamma}_0 \tau G e^{-t/\tau} \qquad \text{(Eq. 16)}$$

The same development as above gives

$$\sigma = \dot{\gamma}_0 \int_{-\infty}^{\infty} \tau H e^{-t/\tau} d\ln \tau \qquad \text{(Eq. 17)}$$

The exponential goes from zero to 1 as τ goes from 1 to infinity. This may be approximated as a step function going from zero to 1 as $t = \tau$, (Alfrey's rule (18)) producing

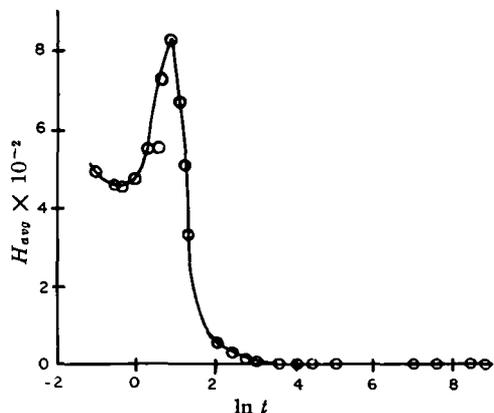$$\sigma = \dot{\gamma}_0 \int_{\ln t}^{\infty} \tau H d\ln \tau \qquad \text{(Eq. 18)}$$

Fig. 4.—A graphical representation of the variation of the average relaxation spectrum with time for 0.30% Carbopol 934 mucilage determined from data obtained from the rising cylinder rheometer.

Differentiation of Eq. 18 leads to (15, 16)

$$-\frac{d\sigma}{d \ln t}\bigg|_{t\,=\,\tau} = \tau\dot{\gamma}_0 H \qquad \text{(Eq. 19)}$$

solving for $H(\tau)$

$$H(\tau = t) = -\frac{1}{\dot{\gamma}_0 t}\frac{d\sigma}{d \ln t} \qquad \text{(Eq. 20)}$$

In the analysis of the relaxation curves of the mucilages, the force in dynes cm.$^{-2}$ was plotted *versus* the natural logarithm of the experimental time and the curve graphically differentiated at each time interval. These differentials were substituted into Eq. 19 along with rate of shear and t to obtain H.

Since no trend was apparent in the value of H obtained for each rate of shear from the rising cylinder data, the values of H at each time interval were averaged to obtain H_{avg} for each mucilage. (An example of the scatter of values of H that go into an H_{avg} is presented in Table III.) H_{avg} was then plotted *versus* $\ln t$ to obtain the form of the relaxation spectrum. A sample plot of the function is found in Fig. 4.

In Eq. 18 $\sigma/\dot{\gamma}_0$ would have the dimensions of viscosity. The integral is designated the dynamic viscosity (17). It has been postulated that dynamic viscosity should be equivalent to plastic viscosity (consistency) for a given shear rate (18, 19). It was therefore decided to obtain dynamic viscosities to compare with previously determined plastic viscosities.

H_{avg} was multiplied by t to give tH_{avg}, and this function was plotted *versus* $\ln t$.

Figure 5 is a sample plot of tH_{avg} *versus* $\ln t$. Graphical integration of these plots of tH_{avg} *versus* $\ln t$ yielded values of dynamic viscosities for the different mucilages. The limits of the integration were from 0.38 seconds at the low end to the time in seconds when the experiment was terminated. In no case was $\ln t$ extrapolated to lower t values than experimentally determined. Values for the dynamic viscosities and plastic viscosities are given in Tables IV and V.

Discussion.—A new viscometer capable of obtaining viscometric data at shear rates comparable with those produced by suspension particles has been developed.
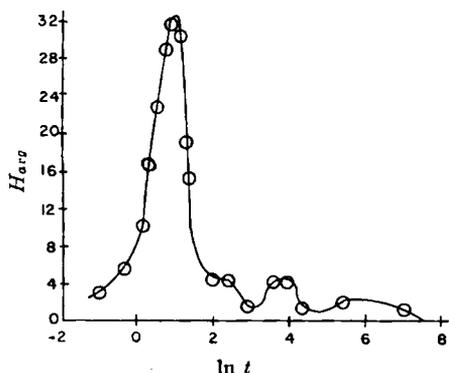

Fig. 5.—A graphical representation of the function from which the dynamic viscosity of 0.15% Carbopol 934 mucilage is obtained from data from the rising cylinder rheometer.

TABLE IV.—DYNAMIC VISCOSITIES OF 2% TRAGACANTH MUCILAGES

Mucilages	Plastic Viscosity, poise	Dynamic Viscosity, poise
No. 1	73.1	149.40
No. 2	39.3	84.00
A	107.1	184.80
Initial	127.7	266.80
Super Initial	501.8	1431.00
Supreme	232.5	719.00

TABLE V.—DYNAMIC VISCOSITIES OF CARBOPOL MUCILAGES

Mucilages, %	Plastic Viscosity, poise	Dynamic Viscosity, poise
0.10	3.5	1.47
0.15	30.2	52.56
0.23	121.3	417.60

The instrument was used for the determination of the viscosities (plastic and apparent), yield values, relaxation spectra, and dynamic viscosities of a series of pharmaceutical suspending agents.

The plastic viscosities and yield values were obtained by fitting the observed points to a straight line by the method of least squares since the points appeared linear. The apparent viscosities were obtained by dividing the shear stress obtained from the line by the corresponding shear rate.

The apparent linearity of the plots is probably misleading. If the dynamic viscosity should be equal to the plastic viscosity (19), the low value obtained from plastic viscosities (Tables IV and V) may be explained by assuming that the flow curves (Fig. 3) are actually concave downward. The need for more experimental work in the low shear region seems established. Accurate prediction of suspension stability must await such comprehensive studies.

REFERENCES

(1) Alfrey, T., Jr., "Mechanical Behavior of High Polymers," Interscience Publishers, New York, N. Y., 1948, p. 34.
(2) McVean, D. E., "Studies in Low Shear Viscometry," Ph.D. dissertation, University of Michigan, Ann Arbor, Mich., 1962, p. 40.
(3) Slattery, J. S., "Non-Newtonian Flow About a Sphere," L. C. card No. Mic. 59-2778, University Microfilms, Inc., Ann Arbor, Mich., 1959.
(4) Pochettino, A., *Nuovo Cimento*, **8**, 77(1914).
(5) Traxler, R. N., Romberg, J. W., and Schweyer, H. E., *Ind. Eng. Chem. Anal. Ed.*, **14**, 340(1942).
(6) Bikermann, J. J., *J. Colloid Sci.*, **3**, 75(1948).
(7) Eirich, F. R., *Proc. Intern. Congr. Holland*, **IV**, 3(1948).
(8) Fox, T. G., Jr., and Flory, P. J., *J. Am. Chem. Soc.*, **70**, 2386(1948).
(9) Lohrenz, J., Swift, G. W., and Kurata, F., *A. I. Ch. E. J.*, **6**, 647(1960).
(10) Bergen, J. T., and Patterson, W., Jr., *J. Appl. Phys.*, **24**, 712(1953).
(11) Bird, R. B., Stewart, W. E., and Lightfoot, E. N., "Transport Phenomena," John Wiley and Sons, Inc., New York, N. Y., 1960, pp. 2–4, 81, 89.
(12) Fox, T. G., Jr., and Flory, P. J., *op. cit.*
(13) Samyn, J. C., and Mattocks, A. M., THIS JOURNAL, **46**, 310(1957).
(14) Maxwell, J. C., *Phil. Mag.*, **35**, 129(1868).
(15) Schremp, F. W., Ferry, J. D., and Evans, W. W., *J. Appl. Phys.*, **22**, 711(1951).
(16) Watkins, J. M., Spangler, R. D., and McKannan, E. C., *ibid.*, **27**, 685(1957).
(17) Leadermann, H., "Rheology, Theory and Applications," Vol. II, edited by Eirich, F. R., Academic Press, Inc., New York, N. Y., 1958, p. 42.
(18) Cox, W. P., and Merz, E. H., *J. Polymer Sci.*, **28**, 619(1958).
(19) Strella, S., *ibid.*, **60**, S9(1962).